ORIGINAL ARTICLE

Human Dose Estimation of [^{64}Cu]Cu-DOTATATE for PET Imaging of Neuroendocrine Tumors

Samaneh Zolghadri [1*], Sara Vosoughi [1], Nafiseh Salek [2], Mohsen Mehrabi [1], Hassan Yousefnia [1]

[1] *Radiation Application Research School, Nuclear Science and Technology Research Institute, Tehran, Iran*

[2] *Nuclear Fuel Research School, Nuclear Science and Technology Research Institute, Tehran, Iran*

*Corresponding Author: Samaneh Zolghadri

Email: szolghadri@aeoi.org.ir

Received: 11 August 2025 / Accepted: 02 January 2026

Abstract

Purpose: This preclinical investigation aimed to evaluate the radiation safety of [^{64}Cu]Cu-DOTATATE through detailed dosimetric assessment, a novel PET radiopharmaceutical targeting Neuroendocrine Tumors (NETs) with overexpression of the SSTR2 receptor, while also exploring its prospective clinical applicability.

Materials and Methods: [^{64}Cu]Cu-DOTATATE was synthesized by radiolabeling DOTATATE with [^{64}Cu]$CuCl_2$, and its radiochemical purity was assessed using HPLC and RTLC. Biodistribution studies were conducted in rats at 2, 4, 12, and 24 h following administration, and radioactivity in the organs was measured with an HPGe detector.

Dosimetric calculations were performed using the MIRD schema, incorporating animal biodistribution data to estimate the absorbed doses in human organs.

Results: [^{64}Cu]Cu-DOTATATE demonstrated excellent radiochemical purity (>99%) and stability over 12 h in PBS and human serum. Biodistribution analysis revealed quick clearance from the blood and significant accumulation in organs that express SSTR2, including the pancreas and adrenal glands, with the kidneys serving as the main route for elimination.

The estimated absorbed doses in key organs were highest in the pancreas (0.21 ± 0.01 mGy/MBq), followed by the kidneys and liver. Comparative dosimetry with other SSTR-targeted agents, like ^{68}Ga-DOTATATE, revealed similar or lower radiation doses in non-target organs.

Conclusion: [^{64}Cu]Cu-DOTATATE exhibited favorable pharmacokinetics and an acceptable radiation dose profile, supporting its potential as a safe and effective PET imaging agent for SSTR2-positive NETs. The extended half-life of ^{64}Cu improves its clinical utility by enhancing tumor-to-background contrast and enabling centralized production, thus facilitating its integration into clinical practice.

Keywords: ^{64}Cu; DOTATATE; Absorbed Dose; Neuroendocrine Tumors.

DOI:

1. Introduction

Neuroendocrine Tumors (NETs) represent a diverse set of cancers that arise from the widespread neuroendocrine system [1, 2]. The clinical management of NETs is challenging due to the frequent occurrence of metastasis and their varied biological behavior [3]. A key molecular hallmark of these tumors is the pronounced overexpression of Somatostatin Receptors (SSTRs), particularly subtype 2 (SSTR2), which has been strategically targeted for both diagnostic imaging and therapeutic applications through the use of radiolabeled Somatostatin Analogs (SSAs) [4].

Peptide Receptor Radionuclide Imaging (PRRI) using ^{68}Ga-labeled somatostatin analogs, such as ^{68}Ga-DOTATATE and ^{68}Ga-DOTATOC, has become the clinical standard for non-invasive detection of SSTR-positive NETs. This method provides exceptional sensitivity and high-quality imaging through Positron Emission Tomography (PET) [5, 6]. However, the short half-life of ^{68}Ga (68 min), coupled with its generator-dependent production, limits its widespread availability, centralized distribution, and the feasibility of delayed imaging protocols [7]. These limitations have led to increased interest in alternative radiometals with longer half-lives, which can be used to develop PET tracers with more flexible logistics and improved dosimetric profiles.

^{64}Cu, with its favorable decay properties (half-life = 12.7 h, β+ emission energy = 653 keV, and a maximum β− emission energy of 579 keV), is considered a leading candidate among radioisotopes [8]. In recent years, it has been applied not only in PET imaging for diagnostics but also in the field of targeted radiotherapy. Its physical and radiochemical characteristics enable delayed imaging (up to 24 h after injection) and centralized production [9, 10]. Today, various radiolabeled compounds based on the ^{64}Cu radioisotope have been developed owing to its suitable physical properties and potential theranostic applications [11, 12]. While some ^{64}Cu-labeled agents such as ^{64}Cu-PSMA-617 and ^{64}Cu-ATSM are now under clinical evaluation [13, 14], ^{64}Cu-DOTATATE has gained significant attention for PET imaging of neuroendocrine tumors.

Clinical studies have demonstrated that [^{64}Cu]Cu-DOTATATE offers high sensitivity and specificity for detecting primary and metastatic NET lesions [15]. A prospective comparison showed that [^{64}Cu]Cu-DOTATATE detected significantly more true-positive lesions than ^{68}Ga-DOTATOC [16]. Not only were more lesions detected, but also ^{64}Cu-DOTATATE provided excellent image contrast at delayed imaging time points up to 24 hours post-injection [15].

Despite its approval and increasing clinical use, the internal radiation burden associated with 64Cu-labeled compounds necessitates detailed preclinical evaluation to characterize biodistribution and calculate organ-specific absorbed doses. These data are essential not only for radiation safety assessments but also for informing the feasibility of theranostic applications using isotopes like ^{67}Cu. Preclinical studies in rodent models provide controlled settings to investigate pharmacokinetics, tumor targeting, and radiation dosimetry, which are critical for supporting translational efforts [17]. The purpose of this research is to carry out a detailed preclinical assessment of ^{64}Cu-DOTATATE, focusing on the analysis of biodistribution and the estimation of absorbed doses.

2. Materials and Methods

The ^{64}Cu was synthesized using a 30 MeV IBA Cyclotron based on the ^{68}Zn(p, αn)^{64}Cu reaction. The DOTATATE peptide and other reagents were sourced from ABX and Sigma-Aldrich Co., respectively. Ion and anion levels were quantified by an Inductively Coupled Plasma Atomic Emission Spectrometer (ICP-AES) with model Optima 7300 DV. To determine radiochemical purity, both thin-layer chromatography with a Bioscan AR2000 scanner and High-Performance Liquid Chromatography (HPLC) (KNAUER-D-14163) were employed. The NIGC-4020 High-Purity Germanium (HPGe) N-type coaxial model was used to quantify radioactivity. The detector exhibited an energy resolution of 1.2 keV (FWHM) at 1332.5 keV (^{60}Co). The full-energy peak efficiency was determined by efficiency calibration using standard gamma reference sources in the same counting geometry as the samples. Statistical analysis was performed using one-way Analysis of Variance (ANOVA) for comparisons across multiple time points, with a significance threshold of $P < 0.05$. All

animal experiments were approved by the Animal Ethics Committee of the Nuclear Science and Technology Research Institute (NSTRI) (Approval No. PRI-B5-00-005) and were conducted in full compliance with institutional guidelines, ethical standards, and applicable national regulations for the care and use of laboratory animals. All procedures were designed in accordance with the principles of the 3Rs (Replacement, Reduction, and Refinement). Animals were housed under controlled environmental conditions (temperature 22 ± 2 °C, 12 h light/dark cycle) with free access to standard laboratory chow and water. At the designated time points, animals were humanely euthanized using CO_2 asphyxiation, in accordance with approved ethical protocols.

2.1. [^{64}Cu]$CuCl_2$ Production and its Quality Control

In this study, enriched ^{68}Zn with a purity of over 98%, obtained from NSTRI, was used for the production of ^{64}Cu. The ^{68}Zn(p,αn) ^{64}Cu reaction was employed, where the proton energy required for the production of 64Cu ranges from 20 to 35 MeV. Due to the energy limitations of the available accelerators (30 MeV), the target needed to be thick enough to reduce the proton energy from 30 MeV to approximately 20 MeV. For this purpose, the target material was electroplated to a thickness of 100 microns on a copper backing. For the synthesis of ^{64}Cu, the ^{68}Zn target was irradiated with protons for 350 µA.h (100 µA for 3.5 h). After irradiation, 10 N hydrochloric acid (HCl) (15 mL) along with hydrogen peroxide (20 µL) was used to dissolve the target. The solution was then processed sequentially through cation and anion exchange columns. To determine the radionuclide purity, an HPGe detector was employed. For assessing radiochemical purity, two distinct solvent systems were used: 1 mM diethylenetriaminepentaacetic acid (DTPA; $C_{14}H_{23}N_3O_{10}$) and a 10% mixture of ammonium acetate and methanol (1:1), with Whatman No. 2 paper and silica gel serving as the stationary phases.

2.2. Preparation, Quality Control, and Stability Studies of [^{64}Cu]Cu-DOTATATE

The preparation of [^{64}Cu]Cu-DOTATATE was carried out based on established protocols from the literature [18]. Briefly, 15 µg of DOTATATE dissolved in distilled water, along with 500 µL of sodium acetate buffer (pH 5.5), were combined with 370 MBq of [^{64}Cu]$CuCl_2$ in a vial.

This mixture was then incubated (95°C, 20 min). The specific activity was calculated as the ratio of the decay-corrected final activity to the molar amount of DOTATATE (15 µg, ≈10.5 nmol), resulting in a specific activity of 35.2 MBq/nmol. HPLC with a C18ODS column (100 mm × 4.6 mm) and RTLC with two phases (ammonium acetate (10%): methanol (30:70), ammonium hydroxide (10%): methanol: water (1:5:10)) were utilized to evaluate the radiochemical purity. The mobile phases of ultrapure water + 1% TFA (A) and acetonitrile (B) were utilized for HPLC analysis. The stability of the final complex was assessed by RTLC at 4, 6, 8, and 12 hours in PBS buffer at 4°C and in fresh human serum (500 µL) at 37°C.

2.3. Biodistribution Studies

The biodistribution study of [^{64}Cu]Cu-DOTATATE was conducted using Sprague-Dawley rats (9±1 weeks, 150±10 g). All experimental protocols followed the ethical guidelines of the 3Rs (Replacement, Reduction, and Refinement). The animals were housed under controlled conditions at 22 ± 2°C with a 12-hour light/dark cycle and had ad libitum access to standard rodent chow and water. Approximately 5.55 ± 0.56 MBq (150 µL) of the complex was administered intravenously via the tail vein.

The activity of syringes was measured both full and empty to ensure accurate delivery of the dose. To investigate biodistribution, the animals were euthanized at specified time intervals following injection. At each specified time point, the following organs were collected: lungs, bones, muscle, kidneys, pancreas, intestines, heart, blood, spleen, stomach, and liver. After thorough washing, each organ was weighed, and the radioactivity was measured using an HPGe detector. The radioactivity levels in each organ were then calculated by Equation 1.

$$A = \frac{N}{\varepsilon\, \gamma\, ts\, k1\, k2\, k3\, k4\, k5} \qquad (1)$$

Where ε and γ represent the detection efficiency and emission probability, respectively. The variable ts denotes the live time, and m refers to the sample mass in kg.

The correction factors, k1 to k5, address several aspects: radioactive decay between the sample collection and the start of measurement (k1), decay during the counting period (k2), self-attenuation within the sample (k3), pulse losses due to random summing (k4), and coincidence effects (k5). N represents the corrected net peak area of the corresponding photopeak, which is calculated as follows Equation 2:

$$N = Ns\frac{ts}{tb}\,Nb \qquad (2)$$

In this Equation, Ns represents the net peak area from the sample spectrum, and Nb is the net peak area from the background spectrum. The variable ts indicates the live time (in seconds) during which the background spectrum was acquired.

The dose percentage per gram of tissue was then calculated using Equation 3, where Total Activity refers to the total amount of radioactivity injected, and m represents the mass of the organ [19, 20].

$$\%\,ID/g = \left(\frac{Activity_{Organ}}{Activity_{Total}}\right) \times 100/m_{Organ} \qquad (3)$$

2.4. Integrated Activity

For calculating the time-integrated activity in human source organs, biodistribution data from rats have been used. According to Equation 4, the time-integrated activity in each organ is calculated as follows:

$$\tilde{A} = \int_0^{\infty} A(t)dt \qquad (4)$$

In this equation, A(t) represents the activity of each organ at time t. The biodistribution data obtained from rat experiments were used to calculate the time-integrated activity in the rat organs. These data were collected at 2, 4, 12, and 24 hours after the injection of the copper radionuclide. These data were then fitted to an exponential function, using the physical decay constant of the copper radionuclide, and extended to infinity.

The calculation of the time-integrated activity in the rat organs was performed using a two-phase combined method. In the first phase, experimental biodistribution data were collected at four time points (2, 4, 12, and 24 h post-injection). These data were corrected and normalized to the actual injected activity. The area under the activity-time curve from 0 to 24 h was calculated using the trapezoidal integration method, with the assumption that the activity at time t=0 was zero for all organs except for blood.

In the second phase, from 24 h to infinity, an exponential decay function was fitted as follows Equation 5 (Figure 1):

$$A(t)=De^{-\lambda t} \qquad (5)$$

In this equation, D represents the experimental data at 24 h, and λ is the physical decay constant of the copper radionuclide. The tail area of the curve was then calculated analytically, and the final value of the time-integrated activity was obtained as the sum of both parts [21-23].

2.5. Extrapolation to Humans

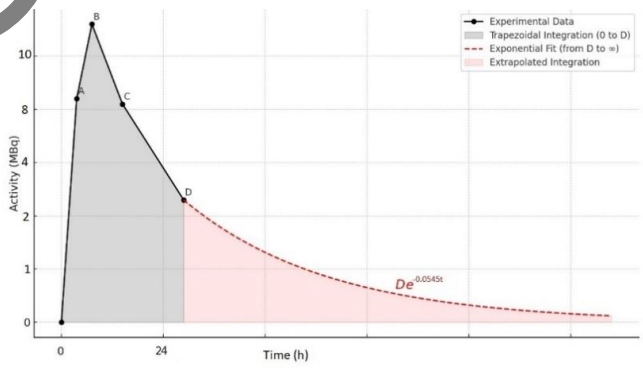

Figure 1. Graph showing time-integrated activity calculation in rat organs. The trapezoidal integration (gray area) covers 0-24 hours, while the exponential decay fit (red dashed line) extrapolates from 24 h to infinity

To estimate the time-integrated activity in human organs, a mass extrapolation method was used, as shown in Equation (6):

$$\bar{A}_{Human\ organ} = \bar{A}_{Animal\ organ} \times \frac{\frac{Organ\ mass_{Human}}{Body\ mass_{Human}}}{\frac{Organ\ mass_{Animal}}{Body\ mass_{Animal}}} \qquad (6)$$

For the initial estimation of human absorbed doses, it was assumed that the biokinetic behavior of the complex in rodents would closely resemble that in humans. This assumption is grounded in the reported similarities between the uptake and clearance mechanisms in both species, as outlined in the ICRP publication [24].

In this study, to ensure accurate estimation, the organ masses of rats and humans were carefully compared. For rats, the organ masses were determined by weighing, while for humans, data from scientific articles and available sources were used. For example, the organ masses for a 70 kg human are provided in Table 1 of the article [25].

Table 1. Exact organ weights for a 70 kg human are provided in the table below

Organ	Human Mass (g)
Bone	6120
Heart	316
Stomach	158
Kidneys	229
Small Intestine	1100
Spleen	183
Muscles	28000
Liver	1910
Lungs	1000
Total Body	73700

2.6. Dose Estimation

The absorbed dose for each target organ in humans was calculated using the MIRD model, as described in Equation 7 [26]

$$\tilde{D}(r_k) = \Sigma_h \tilde{A}_h S(r_{k\leftarrow}r_h) \quad (7)$$

In this equation, $\tilde{A}_h$ represents the total integrated activity over time within a human source organ, and $S(r_{k\leftarrow}r_h)$ refers to the specific S-value associated with the target organ. The S-value incorporates factors such as the radionuclide's physical decay properties, the emission ranges of radiation, and the size and shape of the organs, with units expressed as mGy/MBq.s. For the calculations, the S-values of this study were sourced from the OLINDA/EXM software [27].

2.7. Statistical Analysis

For each time point, four rats were included in the study. Biodistribution data across multiple time points (2, 4, 12, and 24 h) were analyzed using one-way analysis of variance (ANOVA), as independent groups of animals were used at each time interval. Data are presented as mean ± Standard Deviation (SD), and p-values less than 0.05 were considered statistically significant.

The uncertainty associated with absorbed dose estimation was evaluated using a standard error propagation approach. The total uncertainty of the absorbed dose was calculated by combining the uncertainties arising from the time-integrated activity (Ã) and the S-values, according to Equation 8. This method accounts for uncertainties related to curve fitting of time–activity data, numerical integration of the activity–time curves, and S-value estimation. The final absorbed dose uncertainty for each organ was obtained by propagating these individual uncertainty components, and the results are reported as SD in the dosimetry tables [21].

$$\sigma_D^2 = \left(\frac{\sigma_D}{\sigma_{\tilde{A}}}\right)^2 \sigma_{\tilde{A}}^2 + \left(\frac{\sigma_D}{\sigma_S}\right)^2 \sigma_S^2 \quad (8)$$

3. Results

3.1. Preparation and Quality Control of [^{64}Cu]$CuCl_2$

The radionuclidic purity of [^{64}Cu]$CuCl_2$ was determined using an HPGe. The spectrum revealed three main energy peaks at 278 keV (9%), 511 keV (35%), and 1346 keV (1%), all of which were attributed exclusively to copper-64. The absence of additional peaks confirmed a radionuclidic purity of more than 99.9% (Figure 2). Chemical purity analysis, conducted using polarographic methods, showed that the concentrations of copper and zinc in the final product were both below 1 ppm, well within acceptable limits and unlikely to interfere with peptide labeling.

To assess the radiochemical purity of [^{64}Cu]$CuCl_2$, two separate solvent systems were used: a mixture of ammonium acetate (10%) and methanol in equal proportions (1:1), and a solution of DTPA (1 mM). In a 1 mM DTPA system with Whatman No. 2 paper, free copper-64 forms a Cu-DTPA complex that migrates upward with an Rf value of 0.8, while other copper species remain at the origin. In the second system, a

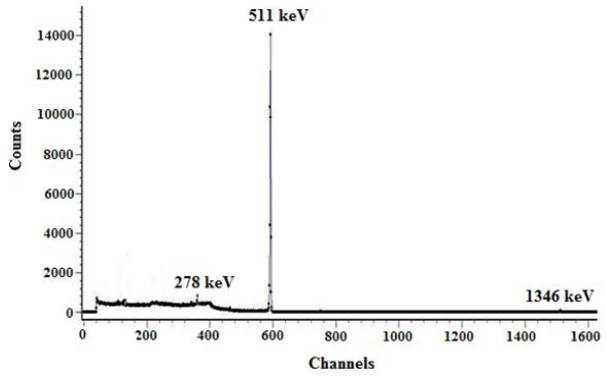

Figure 2. HPGe spectrum of [^{64}Cu]$CuCl_2$. No additional γ-peaks attributable to radionuclidic impurities were observed above background, confirming a radionuclidic purity >99.9% under the measurement conditions

10% ammonium acetate: methanol mixture on a silica gel plate, free copper-64 remains at the origin with an Rf of 0.1, while other chemical species and impurities travel up the plate (Figure 3). The differing impurity patterns observed between these two methods suggest the presence of contaminants in the sample. Overall, the radiochemical purity of the Cu^{2+} ion was found to be greater than 99%.

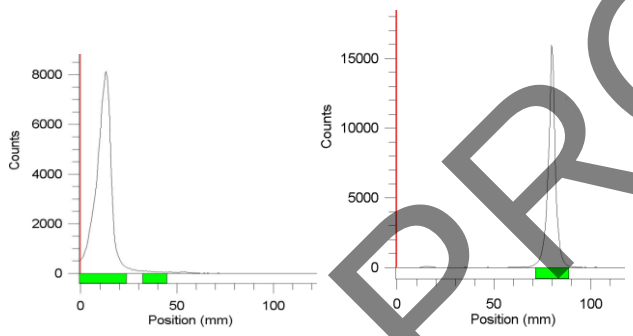

Figure 3. The chromatogram of [^{64}Cu]$CuCl_2$, 10% ammonium acetate: methanol in a (1:1) ratio on silica gel (left chart) and 1mM DTPA and Whatman No. 2 paper (right chart)

3.2. Preparation, Quality Control, and Stability Studies of [^{64}Cu]Cu-DOTATATE

The radiochemical purity of the complex preparation was evaluated using RTLC and HPLC techniques. For RTLC, two different solvent systems were used: (i) ammonium hydroxide, methanol, and water (1:5:10, v/v), and (ii) a 10% ammonium acetate mixed with methanol (30:70, v/v) (Figure 4). In both systems, free copper-64, owing to its higher polarity, remained stationary at the origin, whereas the radiolabeled peptide, being less polar, migrated upward and displayed higher Rf values. This mobility contrast allowed for clear separation between the free radionuclide and the labeled compound, enabling precise assessment of product purity.

In the HPLC analysis, the polar free copper-64 eluted from the column during the early min, whereas the less polar radiolabeled peptide was detected by the detector approximately 9 min after the start of the elution (Figure 5). The radiochemical yield of the labeling reaction, as determined by RTLC and HPLC analyses, was greater than 99%.

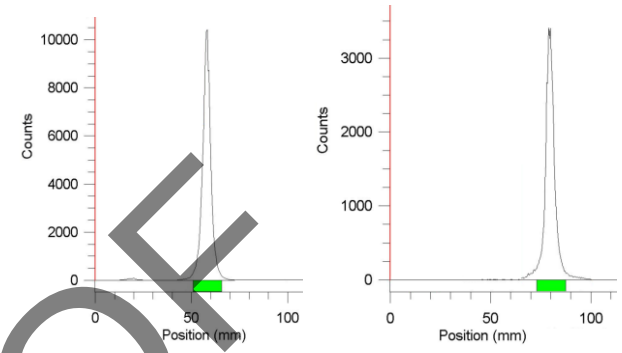

Figure 4. The chromatogram of ^{64}Cu- DOTATATE, ammonium hydroxide: methanol: water mobile phase (1:5:10) on silica gel paper (left chart) and 10% ammonium acetate: methanol mobile phase (30:70) on Whatman No. 2 paper (right chart)

The stability of [^{64}Cu]Cu-DOTATATE was evaluated in PBS buffer (stored at 4°C) and in human serum by monitoring its radiochemical purity over time. The results demonstrated that even after 12 h, the radiochemical purity of complex higher than 90%, indicating its high stability.

3.3. Biodistribution Studies

The biodistribution of the complex was investigated in animals at 2, 4, 12, and 24 h after administration. The uncorrected decay data are shown in Figure 6. As illustrated, the radiopharmaceutical is rapidly eliminated from the bloodstream. Notable accumulation of the tracer occurs in organs with a high density of somatostatin receptors, such as the pancreas, demonstrating targeted uptake. Significant retention of the tracer is also observed in the stomach.

Furthermore, the pronounced uptake in the kidneys, along with increased activity detected in the urine, indicates that the urinary system is the primary pathway for eliminating this radiolabeled peptide, a trend commonly seen in peptide-based radiopharmaceuticals.

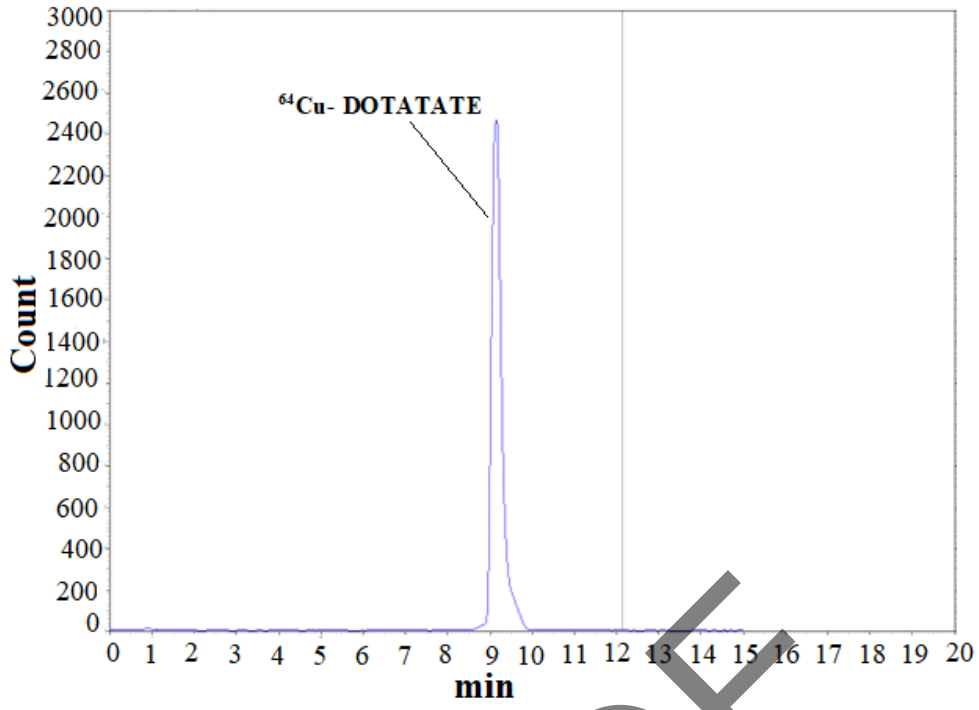

Figure 5. The HPLC chromatogram of the final ^{64}Cu-DOTATATE product

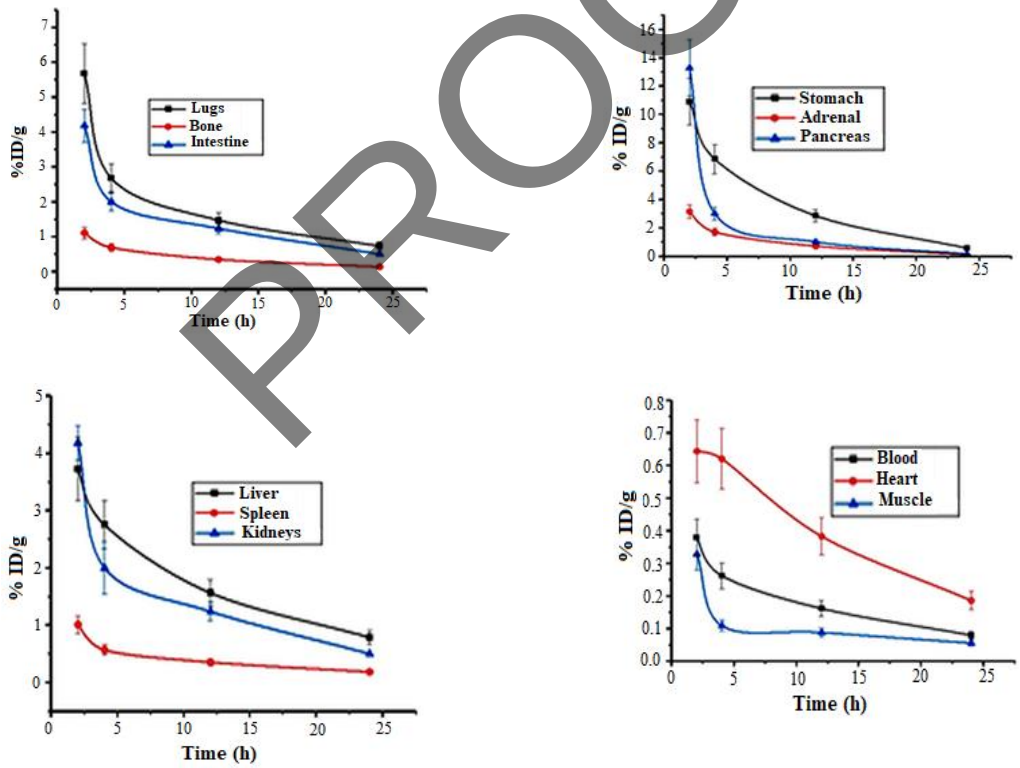

Figure 6. The relative activity concentrations in rats, measured post- injection of [^{64}Cu]Cu-DOTATATE, are presented as the percentage of the injected dose per gram (%ID/g) of tissue, without decay correction. Data are shown as SD (n = 4 animals per time point), and the error bars represent SD. Activity concentrations are plotted as a function of time (h)

3.4. Dose Estimation

The absorbed dose was estimated with the MIRD model for target organs (see Table 2). The pancreas received the highest absorbed dose (0.21 ± 0.01 mGy/MBq), followed by the kidneys, liver, stomach, and Lower wall of the Large Intestine (LLI). Intermediate dose levels were noted in the adrenal glands, gallbladder, and Upper wall of the Large Intestine (ULI), while the doses in other organs were much lower. Statistical analysis showed that the pancreas absorbed a significantly higher dose ($p < 0.05$) compared to the kidneys and liver, supporting the selective accumulation in tissues with SSTR expression.

In this study, a sample size of n=4 per time point was chosen to balance statistical accuracy with practical constraints such as resources, time, and cost. This sample size is commonly used in animal studies with limited sample sizes. A power analysis confirmed that this sample size is sufficient for detecting meaningful differences. This method is appropriate for comparing two independent or paired groups, especially with limited sample sizes and large differences between groups, and it is widely used in similar studies.

Table 2. Estimated organ-absorbed doses (mGy/MBq) in humans following administration of [64Cu]Cu-DOTATATE

Organ	Absorbed dose (mGy/MBq)
Gallbladder	0.08 ± 0.01
Brain	0.00 ± 0.00
Adrenals	0.08 ± 0.01
LLI Wall	0.15 ± 0.01
Small Intestine	0.03 ± 0.00
Stomach	0.10 ± 0.02
Pancreas	0.21 ± 0.02
Red marrow	0.02 ± 0.00
Urine bladder	0.07 ± 0.01
Bone surface	0.05 ± 0.01
Kidney	0.11 ± 0.02
Thymus	0.01 ± 0.00
Lungs	0.04 ± 0.00
ULI wall	0.10 ± 0.02
Heart wall	0.03 ± 0.00
Spleen	0.06 ± 0.01
Liver	0.10 ± 0.02
Total body	0.10±0.02

4. Discussion

Advancements in nuclear medicine, particularly in PET and SPECT imaging technologies, have been accompanied by the development of new radiopharmaceutical agents. These breakthroughs have significantly improved both diagnostic and therapeutic applications. However, they have also raised concerns regarding increased radiation exposure and potential health risks for patients. Consequently, accurate monitoring and control of the absorbed radiation dose have become essential components of clinical practice.

This preclinical study aimed to examine the biodistribution of [64Cu]Cu-DOTATATE and estimate the absorbed dose, evaluating its potential as a PET radiopharmaceutical for targeting SSTR2-positive neuroendocrine tumors. In this study, the radiochemical yield for the synthesis of [64Cu]Cu-DOTATATE was greater than 95%. This yield was calculated by comparing the final activity of the radiopharmaceutical to the primary activity and considered as the radiochemical yield. The radiochemical purity of this compound was assessed using RTLC and HPLC, and its purity was found to be over 99%. These results indicate high efficiency and good quality in the synthesis of [64Cu]Cu-DOTATATE.

Regarding chemical impurities, the main contaminants are metallic ions, primarily due to copper backing and gold substrates in the production process, as well as the use of zinc as a target in the production of [64Cu]$CuCl_2$. These impurities are present at very low levels, with the concentrations of copper and zinc in the final product measured using polarographic methods, showing precise values below 1 ppm.

These levels are well within acceptable limits and do not affect the quality of the radiopharmaceutical.

Concerning radionuclide impurities, using the highly sensitive HPGe detector, the smallest amounts of radionuclide impurities were measured, and the results showed that the radionuclide purity of [64Cu]Cu-DOTATATE was over 99.99%.

The quality control criteria for acceptance or rejection in clinical-scale production of [64Cu]Cu-DOTATATE have been established through

comprehensive evaluations of chemical and radiochemical purity, along with the examination of metallic and radionuclide impurities. These results emphasize that [^{64}Cu]Cu-DOTATATE meets the quality standards required for clinical studies and radiopharmaceutical applications.

The radiolabeled compound demonstrated excellent stability in both human serum and PBS over a 12-h incubation period. The findings indicate that [^{64}Cu]Cu-DOTATATE has favorable pharmacokinetic properties and presents an acceptable radiation dose to non-target tissues. The organ-level absorbed dose estimates (Table 2) further support the observed biodistribution pattern of [^{64}Cu]Cu-DOTATATE. Among SSTR2-rich tissues, the pancreas exhibited the highest absorbed dose (0.21 ± 0.01 mGy/MBq), confirming its role as a primary physiological target organ for somatostatin analog–based radiotracers. Notably, the adrenal glands also demonstrated relatively elevated absorbed doses (0.08 ± 0.00 mGy/MBq), which is consistent with known physiological expression of somatostatin receptors in adrenal tissue and supports receptor-mediated uptake rather than nonspecific accumulation. The kidneys received one of the highest absorbed doses (0.11 ± 0.01 mGy/MBq), identifying them as the dose-limiting organ, in line with the predominant renal clearance pathway of peptide-based radiopharmaceuticals. Intermediate absorbed doses were observed in the liver, stomach, and intestinal walls, reflecting a combination of physiological receptor expression and hepatobiliary or gastrointestinal transit [28]. Consistent with the renal elimination patterns of DOTATATE-based radiopharmaceuticals, significant activity was also detected in the liver and spleen, likely due to the physiological expression of SSTRs and the nonspecific uptake of radiometal-chelate complexes. Additionally, some tracer accumulation was observed in the stomach and intestines, consistent with uptake patterns seen with [^{68}Ga]Ga-DOTATATE [29].

The absorbed dose, estimated using the MIRD and OLINDA/EXM models, reveals a notably high dose in the pancreas, which corresponds to the known overexpression of SSTR in this organ. Likewise, the elevated renal dose is consistent with the typical excretion pattern seen in peptide-based radiopharmaceuticals [30]. As expected, the kidneys, liver, and spleen received significant doses, with values comparable to those observed for other SSTR-targeting agents, including ^{68}Ga-DOTATATE and ^{111}In-pentetreotide (Table 3).

In contrast, the relatively low absorbed doses in other organs indicate that the compound is well distributed, enhancing the potential for [^{64}Cu]Cu-DOTATATE to be considered safe for clinical use.

One of the key advantages of ^{64}Cu over ^{68}Ga is its substantially lower mean positron energy, which results in a shorter positron range and consequently improved spatial resolution in PET imaging (Table 4). A reduced positron range leads to less image blurring and more accurate lesion delineation, particularly for small lesions [33]. This physical property contributes to enhanced image contrast and reduced partial volume effects, as reported in previous clinical studies of ^{64}Cu-DOTATATE. Although the longer half-life of ^{64}Cu may result in a slightly higher effective dose, this diagnostic trade-off is offset by improved diagnostic performance, the capability for delayed imaging, and superior image quality compared with ^{68}Ga-labeled tracers.

Table 3. Comparison of human absorbed doses (mGy/MBq) of [^{64}Cu]Cu-DOTATATE with other radiolabeled compounds used for imaging of SSTR-positive NETs

Target organs	Human Absorbed Dose (mGy/MBq)		
	^{68}Ga-DOTATATE	^{111}In-pentetreotide	[^{64}Cu]Cu-DOTATATE
Kidneys	0.09±0.02	0.52	0.11 ± 0.02
Liver	0.05±0.02	0.07	0.10 ± 0.02
Spleen	0.11±0.06	0.34	0.06 ± 0.01
Pancreas	-	0.06	0.21 ± 0.02
Adrenals	0.09±0.05	0.06	0.08 ± 0.01
Red Marrow	0.02±0.00	0.03	0.02 ± 0.00
Effective dose (mSv/MBq)	0.02±0.00	0.07	0.06±0.02
Reference	[31]	[32]	This study

Table 4. Physical decay properties and imaging characteristics of commonly used radionuclides for imaging

Radionuclide	Decay Mode	Imaging Method	E_{mean} β^+(keV)
^{68}Ga	β^+	PET	836
^{111}In	IT	SPECT	-
^{64}Cu	β^+	PET	278

While these strengths are notable, it is essential to recognize some limitations. First, translating preclinical dosimetry to humans inherently involves uncertainties due to physiological and anatomical differences between species. Although standardized interspecies scaling methods were employed, variations in SSTR expression, tracer kinetics, and organ sizes may influence the clinical applicability of these findings. Although human absorbed dose estimates were derived from rat biodistribution data using a mass-based extrapolation method, it should be acknowledged that interspecies differences in SSTR2 expression and renal clearance mechanisms may influence the accuracy of direct translation. This approach, however, represents a commonly accepted first-order methodology in preclinical dosimetry [34, 35] and is consistent with ICRP recommendations [24]. While more advanced allometric or Physiologically Based Pharmacokinetic (PBPK) models may further refine interspecies extrapolation, such analyses were beyond the scope of the present study. The use of larger animal models could potentially reduce scaling uncertainty but would preclude comprehensive organ dissection and necessitate imaging-based quantification, which introduces additional limitations related to spatial resolution and equipment availability. Therefore, ex vivo biodistribution studies in rodents remain a valuable and dependable approach for estimating human doses at the initial stage.

Second, using healthy animals may not fully reflect the distribution patterns observed in patients with multifocal or metastatic NETs. Future studies using orthotopic or genetically modified models could offer a more accurate representation of the clinical setting.

This statistical approach provides a robust evaluation of time-dependent biodistribution patterns while appropriately controlling for multiple comparisons. Additionally, the limitation of the small sample size (n=4) has been identified. This limitation is significant and may affect the statistical power and generalizability of the results. Therefore, this limitation will be mentioned in the revised manuscript.

It is important to note that the uncertainties in absorbed dose reported in this study account for propagated errors from time-activity curve fitting, numerical integration, and S-values, offering a conservative yet realistic estimation of dosimetric accuracy.

In this study, all biodistribution experiments were conducted in healthy rats, whereas the tracer [^{64}Cu]Cu-DOTATATE is designed for imaging NETs. This represents a limitation, as the expression of SSTR2 in the normal rat pancreas may not reflect tumor uptake behavior. Additionally, the tumor-sink effect can alter systemic distribution and organ doses in tumor-bearing models. Results obtained from healthy animals may slightly differ from clinical uptake or dosimetry patterns in tumor models.

Although this study generally provides reasonable estimations of the absorbed dose in various human organs after the injection of the radiopharmaceutical, tumor studies are recommended for more accurate predictions.

Finally, although this study primarily focused on diagnostic purposes, the increasing interest in copper-based theranostics highlights the need for further exploration of ^{64}Cu/^{67}Cu pairs in therapeutic planning. Due to their similar coordination chemistry and biological behavior, [^{64}Cu]Cu-DOTATATE is an ideal candidate to pair with ^{67}Cu-DOTATATE, potentially enabling more precise image-guided dosimetry and personalized treatment approaches.

5. Conclusion

In conclusion, [^{64}Cu]Cu-DOTATATE demonstrated favorable biodistribution, with rapid clearance from the bloodstream and substantial uptake in SSTR2-positive tissues, particularly the pancreas. The absorbed dose to most organs was relatively low, supporting its safety profile. Given its favorable pharmacokinetics and potential for theranostic applications, [^{64}Cu]Cu-DOTATATE shows considerable promise as a PET imaging agent for the diagnosis and treatment of neuroendocrine tumors. Future research should aim to further validate its

clinical use, particularly in combination with therapeutic isotopes like ^{67}Cu, to advance personalized treatment strategies.

Acknowledgements

The authors would like to acknowledge the Nuclear Science and Technology Research Institute for its support.

References

1- Irvin M Modlin *et al.*, "Gastroenteropancreatic neuroendocrine tumours." *The lancet oncology,* Vol. 9 (No. 1), pp. 61-72, (2008).

2- James C Yao *et al.*, "One hundred years after "carcinoid": epidemiology of and prognostic factors for neuroendocrine tumors in 35,825 cases in the United States." *Journal of clinical oncology,* Vol. 26 (No. 18), pp. 3063-72, (2008).

3- Pamela L Kunz, "Carcinoid and neuroendocrine tumors: building on success." *Journal of clinical oncology,* Vol. 33 (No. 16), pp. 1855-63, (2015).

4- Thomas A Hope *et al.*, "Appropriate use criteria for somatostatin receptor PET imaging in neuroendocrine tumors." *Journal of Nuclear Medicine,* Vol. 59 (No. 1), pp. 66-74, (2018).

5- Marta Opalińska, Karolina Morawiec-Sławek, Adrian Kania-Kuc, Ibraheem Al Maraih, Anna Sowa-Staszczak, and Alicja Hubalewska-Dydejczyk, "Potential value of pre- and post-therapy [68Ga] Ga-DOTA-TATE PET/CT in the prognosis of response to PRRT in disseminated neuroendocrine tumors." *Frontiers in Endocrinology,* Vol. 13p. 929391, (2022).

6- Mojdeh Naderi, Samaneh Zolghadri, Hassan Yousefnia, Ali Ramazani, and Amir Reza Jalilian, "Preclinical study of 68Ga-DOTATOC: Biodistribution assessment in syrian rats and evaluation of absorbed dose in human organs." *Asia Oceania Journal of Nuclear Medicine and Biology,* Vol. 4 (No. 1), p. 19, (2016).

7- Carolyn J Anderson and Riccardo Ferdani, "Copper-64 radiopharmaceuticals for PET imaging of cancer: advances in preclinical and clinical research." *Cancer Biotherapy and Radiopharmaceuticals,* Vol. 24 (No. 4), pp. 379-93, (2009).

8- Anupriya Chhabra and Mathew L Thakur, "Theragnostic radionuclide pairs for prostate cancer management: 64Cu/67Cu, can be a budding hot duo." *Biomedicines,* Vol. 10 (No. 11), p. 2787, (2022).

9- Mathias Loft *et al.*, "64Cu-DOTATATE PET in patients with neuroendocrine neoplasms: prospective, head-to-head comparison of imaging at 1 hour and 3 hours after injection." *Journal of Nuclear Medicine,* Vol. 62 (No. 1), pp. 73-80, (2021).

10- Abhishek Jha *et al.*, "Choice Is Good at Times: The Emergence of [64Cu] Cu-DOTATATE–Based Somatostatin Receptor Imaging in the Era of [68Ga] Ga-DOTATATE." *Journal of Nuclear Medicine,* Vol. 63 (No. 9), p. 1300, (2022).

11- Jason P Holland, Riccardo Ferdani, Carolyn J Anderson, and Jason S Lewis, "Copper-64 radiopharmaceuticals for oncologic imaging." *PET clinics,* Vol. 4 (No. 1), pp. 49-67, (2009).

12- Samaneh Zolghadri, Fateme Badipa, Hassan Yousefnia, and Zahra Shiri-Yekta, "Development of [64Cu] Cu-BPAMD for PET imaging of bone metastases." *Radiochimica Acta,* Vol. 112 (No. 4), pp. 247-53, (2024).

13- Bernhard Grubmueller *et al.*, "64Cu-PSMA-617 PET/CT imaging of prostate adenocarcinoma: first in-human studies." *Cancer Biotherapy and Radiopharmaceuticals,* Vol. 31 (No. 8), pp. 277-86, (2016).

14- Kimiteru Ito *et al.*, "Phase I Study of 64Cu-ATSM Therapy in Malignant Brain Tumors: Safety, Pharmacokinetics, and Preliminary Outcomes." ed: Society of Nuclear Medicine, (2025).

15- Andreas Pfeifer *et al.*, "Clinical PET of neuroendocrine tumors using 64Cu-DOTATATE: first-in-humans study." *Journal of Nuclear Medicine,* Vol. 53 (No. 8), pp. 1207-15, (2012).

16- Camilla B Johnbeck *et al.*, "Head-to-head comparison of 64Cu-DOTATATE and 68Ga-DOTATOC PET/CT: a prospective study of 59 patients with neuroendocrine tumors." *Journal of Nuclear Medicine,* Vol. 58 (No. 3), pp. 451-57, (2017).

17- Haochuan Guo *et al.*, "The pivotal role of preclinical animal models in anti-cancer drug discovery and personalized cancer therapy strategies." *Pharmaceuticals,* Vol. 17 (No. 8), p. 1048, (2024).

18- Samaneh Zolghadri, Fateme Badipa, Naeimeh Amraee, Behrouz Alirezapour, Davood Beiki, and Hassan Yousefnia, "Development and evaluation of [64Cu] Cu-DOTATATE for clinical applications." *Iranian Journal of Nuclear Medicine,* Vol. 31 (No. 2), pp. 157-66, (2023).

19- Saeid Ranjbar, Seyed Mahmoud Reza Aghamiri, Saeed Rajabifar, Samaneh Zolghadri, and Hassan Yousefnia, "[113mIn] In-RM2: a high potential agent for

SPECT imaging of GRPR-expressing tumors." *Physical and Engineering Sciences in Medicine,* Vol. 48 (No. 1), pp. 273-83, (2025).

20- Leyla Akbari, Sedigheh Sina, Samaneh Zolghadri, Ali Moghaddasi, Kamal Hadad, and Hassan Yousefnia, "[113mIn] In-PSMA: high potential agent for SPECT imaging of prostate cancer." *Radiochimica Acta,* Vol. 112 (No. 11), pp. 883-94, (2024).

21- Samaneh Zolghadri, Saeed Ranjbar, Fateme Taati, Arezou Karimian, Hassan Yousefnia, and Yohannes Sardjono, "Human dose estimation of a novel SPECT imaging agent using animal experimental data and Monte Carlo simulation." *Radiation and Environmental Biophysics,* pp. 1-14, (2025).

22- Samaneh Zolghadri, Fatemeh Mohammadpour-Ghazi, and Hassan Yousefnia, "Preclinical studies and absorbed dose estimation of [89Zr] Zr-DFO-Bevacizumab for PET imaging of VEGF-expressing tumors." *Applied Radiation and Isotopes,* Vol. 210p. 111379, (2024).

23- Eun Young Han, Wesley E Bolch, and Keith F Eckerman, "Revisions to the ORNL series of adult and pediatric computational phantoms for use with the MIRD schema." *Health Physics,* Vol. 90 (No. 4), pp. 337-56, (2006).

24- ICRP ICRP, "Radiological protection in biomedical research." *ICRP Publication,* Vol. 62(1992).

25- Hassan Yousefnia, Samaneh Zolghadri, Amir Reza Jalilian, Mojtaba Tajik, and Mohammad Ghannadi-Maragheh, "Preliminary dosimetric evaluation of 166Ho-TTHMP for human based on biodistribution data in rats." *Applied Radiation and Isotopes,* Vol. 94pp. 260-65, (2014).

26- Walter Stephen Snyder, "" S" absorbed dose per unit cumulated activity for selected radionuclides and organs." *MIRD Pamphlet no. 11,* (1975).

27- Michael G Stabin, Richard B Sparks, and Eric Crowe, "OLINDA/EXM: the second-generation personal computer software for internal dose assessment in nuclear medicine." *Journal of Nuclear Medicine,* Vol. 46 (No. 6), pp. 1023-27, (2005).

28- Flavio Forrer *et al.*, "A comparison of 111In-DOTATOC and 111In-DOTATATE: biodistribution and dosimetry in the same patients with metastatic neuroendocrine tumours." *European journal of nuclear medicine and molecular imaging,* Vol. 31 (No. 9), pp. 1257-62, (2004).

29- Salih Özgüven *et al.*, "Physiological biodistribution of 68Ga-DOTA-TATE in normal subjects." *Molecular imaging and radionuclide therapy,* Vol. 30 (No. 1), p. 39, (2021).

30- Hassan Yousefnia, Masoumeh-Sadat Mousavi-Daramoroudi, Samaneh Zolghadri, and Fereydoun Abbasi-Davani, "Preparation and biodistribution assessment of low specific activity 177 Lu-DOTATOC for optimization studies." *Iranian Journal of Nuclear Medicine,* Vol. 24 (No. 2), (2016).

31- Mattias Sandström *et al.*, "Comparative biodistribution and radiation dosimetry of 68Ga-DOTATOC and 68Ga-DOTATATE in patients with neuroendocrine tumors." *Journal of Nuclear Medicine,* Vol. 54 (No. 10), pp. 1755-59, (2013).

32- MG Stabin *et al.*, "Radiation dosimetry for indium-111-pentetreotide." *Journal of Nuclear Medicine,* Vol. 38 (No. 12), pp. 1919-22, (1997).

33- Ulrich Knigge Camilla B Johnbeck , Annika Loft , *et al.*, "Head-to-Head Comparison of 64Cu-DOTATATE and 68Ga-DOTATOC PET/CT: A Prospective Study of 59 Patients with Neuroendocrine Tumors." *Journal of Nuclear Medicine,* Vol. 53 (No. 3), pp. 451-57, (2016).

34- Wei-Ann Hsueh Adam L. Kesner, Johannes Czernin, Henry Padgett, Michael E. Phelps & Daniel H. S. Silverman, "Radiation Dose Estimates for [18F]5-Fluorouracil Derived from PET-Based and Tissue-Based Methods in Rats." *Molecular Imaging and Biology,* Vol. 10pp. 341–48, (2008).

35- Edalat Radfar, Amir R. Jalilian, Hassan Yousefnia, Ali Bahrami-samani, and Mohammad Ghannadi-Maragheh, "A comparative study of preliminary dosimetry for human based on distribution data in rats with 111In, 90Y, 153Sm, and 177Lu labeled rituximab. ." *Nuclear Technology and Radiation Protection,* Vol. 27 (No. 2144-151), (2012).